MOLECULAR AND CELLULAR BIOLOGY, Oct. 2004, p. 8342–8355 Vol. 24, No. 19
0270-7306/04/$08.00+0 DOI: 10.1128/MCB.24.19.8342–8355.2004

Swi1 and Swi3 Are Components of a Replication Fork Protection Complex in Fission Yeast

Eishi Noguchi,[1]* Chiaki Noguchi,[1] W. Hayes McDonald,[2] John R. Yates III,[2] and Paul Russell[1,2]*

Departments of Molecular Biology[1] and Cell Biology,[2] The Scripps Research Institute, La Jolla, California

Received 5 February 2004/Returned for modification 17 March 2004/Accepted 29 June 2004

Swi1 is required for programmed pausing of replication forks near the *mat1* locus in the fission yeast *Schizosaccharomyces pombe*. This fork pausing is required to initiate a recombination event that switches mating type. Swi1 is also needed for the replication checkpoint that arrests division in response to fork arrest. How Swi1 accomplishes these tasks is unknown. Here we report that Swi1 copurifies with a 181-amino-acid protein encoded by *swi3*$^+$. The Swi1-Swi3 complex is required for survival of fork arrest and for activation of the replication checkpoint kinase Cds1. Association of Swi1 and Swi3 with chromatin during DNA replication correlated with movement of the replication fork. *swi1*Δ and *swi3*Δ mutants accumulated Rad22 (Rad52 homolog) DNA repair foci during replication. These foci correlated with the Rad22-dependent appearance of Holliday junction (HJ)-like structures in cells lacking Mus81-Eme1 HJ resolvase. Rhp51 and Rhp54 homologous recombination proteins were not required for viability in *swi1*Δ or *swi3*Δ cells, indicating that the HJ-like structures arise from single-strand DNA gaps or rearranged forks instead of broken forks. We propose that Swi1 and Swi3 define a fork protection complex that coordinates leading- and lagging-strand synthesis and stabilizes stalled replication forks.

Accurate replication of the millions or billions of DNA base pairs in a eukaryotic genome is a remarkable achievement. This accomplishment is even more astonishing when one considers that the conditions for DNA synthesis are rarely ideal. Damaged templates, protein complexes bound to DNA, and inadequate supplies of deoxyribonucleotide triphosphates (dNTPs) are among the many obstacles that must be overcome to replicate a genome. All of these situations can stall replication forks. Stalled forks pose grave threats to genome integrity because they can rearrange, break, or collapse through disassembly of the replication complex (36).

Preserving genome integrity when forks stall is in large part the responsibility of the replication checkpoint (10, 44). The protein kinase Cds1 is a critical effector of the replication checkpoint in the fission yeast *Schizosaccharomyces pombe* (7, 31). One of its major functions is to prevent the onset of mitosis by regulating mitotic control proteins, but perhaps its most important activity is to stabilize replication forks (10). Cds1 is required to prevent fork breakage in cells treated with hydroxyurea (HU), a ribonucleotide reductase inhibitor that stalls replication by depleting dNTPs (41). In the budding yeast *Saccharomyces cerevisiae*, a failure to activate Rad53, a Cds1 homolog, is associated with collapse and regression of replication forks and gross chromosomal rearrangements in cells treated with HU (29, 33, 55, 58).

Replication checkpoint studies have typically used chemical agents or DNA replication mutants to stall replication, but there is abundant evidence of natural replication pause and termination sites (60). One of the best-characterized examples involves cell differentiation in fission yeast. Programmed fork pausing and termination events near the mating-type (*mat1*) locus in fission yeast are needed to create an imprint, probably a DNA strand discontinuity, that initiates a gene conversion event that switches mating type (13, 26). These events require *swi1*$^+$ and *swi3*$^+$. Swi1 has been identified (13) and shown to be required for proficient activation of Cds1 (41). Cds1 is not required for mating-type switching, thus Swi1 has both Cds1-dependent and -independent activities. A similar situation exists in budding yeast. Tof1, a Swi1 homolog, is involved in control of Rad53 (17). Tof1 travels with the replication fork and is needed to restrain fork progression when DNA synthesis is inhibited by HU (25). This function is shared with Mrc1, another protein involved in Rad53 activation (25, 43). Curiously, *tof1*Δ mutants are only weakly sensitive to HU (17), indicating that budding yeast readily tolerates uncoupling of replisome movement and DNA synthesis.

Swi1 is required for proficient DNA replication in the absence of agents that cause genotoxic stress (41). *swi1*Δ mutants accumulate foci containing the Rad22 DNA repair protein during S phase. Relatively fewer Rad22 foci appear in *cds1*Δ mutants, indicating that replication abnormalities in *swi1*Δ cells are not associated with an inability to activate Cds1. Mus81-Eme1, a DNA endonuclease implicated in cleavage of cruciform DNA structures such as Holliday junctions (HJs) and nicked HJs (8, 19, 45), is vital for survival in *swi1*Δ mutants (41). Mus81 is not required for viability in *cds1*Δ cells (9). These findings, coupled with evidence that Swi1 associates with chromatin specifically in S phase, led us to propose that Swi1 travels with the replisome and stabilizes stalled forks in a

* Corresponding author. Present address for Eishi Noguchi: Department of Biochemistry, MS497, Drexel University College of Medicine, 245 N. 15th St., Philadelphia, PA 19102. Phone: (215) 762-4825. Fax: (215) 762-4452. E-mail: Eishi.Noguchi@drexel.edu. Mailing address for Paul Russell: Department of Molecular Biology, MB-3, The Scripps Research Institute, 10550 North Torrey Pines Rd., La Jolla, CA 92037. Phone: (858) 784-8273. Fax: (858) 784-2265. E-mail: prussell@scripps.edu.

configuration that is recognized by the replication checkpoint (41).

Swi1 and Tof1 belong to a large protein family that was first defined by metazoan Tim1 (*Timeless*) (12, 13, 41). *Drosophila melanogaster* and mammalian Tim1s are implicated in circadian rhythmic oscillation (5), whereas the *Caenorhabditis elegans* Tim1 is required for proper chromosome cohesion and segregation (12). It is curious that members of the same protein family should appear to have such diverse functions. To better understand this protein family, we have identified proteins that interact with Swi1. Here we report that Swi1 has a tight association with a small conserved protein that we show is encoded by *swi3*$^+$. Our studies suggest that mutants defective for the Swi1-Swi3 complex accumulate single-strand DNA (ssDNA) gaps during DNA replication that can recombine to form HJs. We propose that the Swi1-Swi3 heterodimer defines an evolutionarily conserved fork protection complex (FPC) that coordinates leading- and lagging-strand synthesis. This activity is required for accurate DNA replication, fork protection, and replication checkpoint signaling.

MATERIALS AND METHODS

General techniques. Methods for genetic and biochemical analyses of fission yeast have been described elsewhere (2, 37). For immunoblotting, extracts from ~1 × 10^8 cells were made by glass bead disruption in lysis buffer A (50 mM Tris-HCl [pH 8.0], 150 mM NaCl, 0.1% NP-40, 10% glycerol, 50 mM NaF, 1 mM Na_3VO_4, 5 mM EDTA, 5 mM *N*-methylmaleimide, 1 μM microcystin, 0.1 μM okadaic acid, and 1 mM dithiothreitol) supplemented with protease inhibitors (0.2 mM *p*-4-amidoinophenyl-methane sulfonyl fluoride hydrochloride monohydrate [*p*-APMSF] and Roche protease inhibitor cocktail). Protein extracts were clarified by centrifugation at 15,000 × *g* for 10 min at 4°C. For small-scale TAP tag protein precipitation, protein extracts were mixed with immunoglobulin G-Sepharose beads and incubated for 2 h at 4°C. The Sepharose beads were collected and washed three times in lysis buffer A. Proteins associated with the beads were analyzed by immunoblotting. Immunoblotting methods and Cds1 kinase assays have been described previously (31, 57). In situ chromatin binding assays were carried out as described elsewhere (27). To calculate a green fluorescent protein (GFP) signal value in live cells, we measured the total GFP signal intensity of an 81-pixel region in the nucleus by using IPlab software (Scanalytics Inc.). The total GFP signal intensity was divided by 81 to obtain a GFP signal value per pixel. Twenty-five nuclei from each strain were measured to obtain the average GFP signal value and standard deviation. Mating-type switching assays were performed as described elsewhere (21). For the UV sensitivity assay, cells were exposed to short-wavelength (254-nm) UV in a Stratalinker (Stratagene, La Jolla, Calif.). To visualize nuclear DNA and the cell wall, cells were fixed in 2.5% glutaraldehyde for 20 min on ice. Cells were washed in phosphate-buffered saline and stained with 4′,6-diamidino-2-phenylindole (DAPI).

Identification of Swi3. Cells expressing Swi1-TAP at its own genomic locus were cultured in 8 liters of yeast extract supplemented (YES) medium until an optical density at 600 nm of 1.2 was reached, and cells were collected. Cell lysate was prepared by grinding a cell pellet that was frozen in lysis buffer B (50 mM Tris-HCl [pH 8.0], 150 mM NaCl, 0.1% NP-40, 10% glycerol, 50 mM NaF, 0.1 mM Na_3VO_4, 5 mM EDTA, 60 mM β-glycerophosphate, 15 mM *p*-nitrophenyl phosphate, and 1 mM dithiothreitol) supplemented with protease inhibitors (0.2 mM *p*-APMSF and Roche protease inhibitor cocktail) as described previously (8). Clarified cell extract was obtained by high-speed centrifugation at 30,000 rpm at 4°C in a Ti35 rotor for 1 h and filtration through a 0.45-μm-pore-size filter. Swi1-TAP and associated proteins were purified and trichloroacetic acid precipitated as described elsewhere (8, 50). The precipitated sample was analyzed by multidimensional protein identification technology (MudPIT) as described previously (8).

ChIP assay. Chromatin immunoprecipitation (ChIP) was performed basically as described elsewhere (42). *S. pombe* cells (5 × 10^8) were fixed in 1% formaldehyde for 20 min at room temperature and quenched in 125 mM glycine for 5 min. Cells were washed in Tris-buffered saline and disrupted in lysis buffer (50 mM HEPES-KOH [pH 7.5], 140 mM NaCl, 1 mM EDTA, and 1% Triton X-100) supplemented with protease inhibitors (0.2 mM *p*-APMSF and Roche protease inhibitor cocktail). The broken cells were sonicated six times for 20 s each until chromatin DNA was sheared into 500- to 700-bp fragments. Cell lysate was clarified by two rounds of maximum-speed centrifugation in an Eppendorf 5415C microcentrifuge at 4°C. Immunoprecipitation was performed on the clarified lysate with anti-FLAG M2 agarose (Sigma) or anti-myc 9E10 antibody bound to protein G-Sepharose. PCR amplification and primers used in these studies have been described previously (42).

Branch migration experiments and 2D gel electrophoresis. Two-dimensional (2D) gel electrophoresis was performed as described elsewhere (11, 28). Cells grown in YES medium were arrested with 0.1% sodium azide and chilled on ice for 5 min. Approximately 2 × 10^9 cells were harvested and washed with ice-cold water before storage at −80°C. Genomic DNA was purified as described elsewhere (41, 53). Samples of 5 μg of DNA were digested with 30 U each of HindIII and KpnI. Precipitated DNA was run on a 0.4% agarose gel in the first dimension. The gel slice of the first-dimension electrophoresis was incubated in branch migration buffer (10 mM Tris-HCl [pH 8.0], 0.1 M NaCl, and 0.1 mM EDTA) as described elsewhere (6, 19, 53, 70) at 4 or 65°C for 5 h. The gel slice was then processed for the second dimension of electrophoresis in a 1% gel. After electrophoresis, the DNA was transferred to a Hybond N^+ membrane (Amersham Biosciences). Hybridization was carried out with the 3-kb HindIII-KpnI radiolabeled ribosomal DNA (rDNA) fragments (68). Radioactive signals were detected using a Molecular Dynamics Storm 840 instrument.

Gene cloning, plasmids, and *S. pombe* strain construction. The 1.2-kb *swi3*$^+$ genomic fragment was amplified by KOD-XL polymerase (Novagen) and introduced into the BamHI/SmaI site of pAL-sk, resulting in pAL-swi3. Plasmids pAL-cds1 and pAL-swi1 have been described elsewhere (41). *swi3* cDNA was amplified from the *S. pombe* cDNA library with EXtaq polymerase (TaKaRa) and subcloned into the pBluescript II vector. Sequencing analysis of *swi3* cDNA revealed that *swi3*$^+$ has an additional exon in the 5′ region of the annotated open reading frame, SPBC30D10.04. Swi3 nucleotide and protein sequence data are available in the DDBJ, EMBL, and GenBank databases, with the accession number AY498547. *swi1*Δ (*swi1*::*Kan*^{r}) was generated by a two-step PCR-based method (30) using primers P73, P74, P77, and P78. *swi1-TAP* (*swi1-TAP*::*Kan*^{r}), *swi1-13myc* (*swi1-13myc*::*Kan*^{r}), *swi1-GFP* (*swi1-GFP*::*Kan*^{r}), and *swi1-3FLAG* (*swi1-3FLAG*::*Kan*^{r}) were generated by a two-step PCR method (30) using primers P75, P76, P77, and P78 to place epitope tags at the C terminus of *swi1*. *swi3*Δ (*swi3*::*Kan*^{r}) was generated by a two-step PCR method (30) using primers P280, P285, P287, and P282. *swi3-TAP* (*swi3-TAP*::*Kan*^{r}), *swi3-13myc* (*swi3-13myc*::*Kan*^{r}), *swi3-GFP* (*swi3-GFP*::*Kan*^{r}), and *swi3-3FLAG* (*swi3-3FLAG*::*Kan*^{r}) were generated by a two-step PCR-based method (30) using primers P281, P286, P287, and P282 to place epitope tags at the C terminus of *swi3*. *rad11-3FLAG* (*rad11-3FLAG*:*Kan*^{r}) was generated by a one-step PCR method (4) using primers rpa1-1 and rpa1-2. Plasmids used as templates for PCR-based gene disruption and gene tagging have previously been described for pFA6a-KanMX6 (4), pFA6a-TAP-KanMX6 (8), pFA6a-13myc-KanMX6 (4), and pFA6a-GFP-KanMX6 (4). pFA6a-3FLAG-KanMX6 was constructed by replacing the PacI-AscI GFP fragment in pFA6a-GFP-KanMX6 with a $FLAG_3$ fragment. Primers used for PCR-based gene disruption and gene tagging are available on request.

Mutations and epitope-tagged genes have previously been described for *cdc6-23* (23), *cdc20-M10* (40), *cdc25-22* (16), *swi3-1* (22), *cds1*Δ (*cds1*::*ura4*$^+$) (7), *chk1*Δ (*chk1*::*ura4*$^+$) (3), *rad26*Δ (*rad26*::*ura4*$^+$) (3), *mus81*Δ (*mus81*::*Kan*^{r}) (9), *rad13*Δ (*rad13*::*ura4*$^+$) (69), *uve1*Δ (*uve1*::*LEU2*) (69), *rad22*Δ (*rad22*::*ura4*$^+$) (46), *rhp51*Δ (*rhp51*::*ura4*$^+$) (38), *rhp54*Δ (*rhp54*::*ura4*$^+$) (39), *rqh1*Δ (*rqh1*::*ura4*$^+$) (56), and *rad22-YFP* (*rad22-YFP*:*Kan*^{r}) (15, 41).

***S. pombe* strains.** *S. pombe* strains used in this study were the following: AL2229 (*h*$^+$ *cdc6-23 ade6-210*), BF2115 (*h*$^+$ *cds1*::*ura4*$^+$ *chk1*::*ura4*$^+$), EN3180 (*h*$^-$ *rad26*::*ura4*$^+$), EN3181 (*h*$^+$ *chk1*::*ura4*$^+$), EN3182 (*h*$^-$ *swi1*::*Kan*^{r}), EN3190 (*h*$^+$ *mus81*::*Kan*^{r}), EN3191 (h$^+$ *swi1-GFP*:*Kan*^{r}), EN3192 (*h*$^-$ *swi1*::*Kan*^{r} *mus81*::*Kan*^{r}), EN3197 (*h*^{90} *swi1*::*Kan*^{r}), EN3222 (*h*$^-$ *rad22-YFP*:*Kan*^{r}), EN3286 (*rad13*::*ura4*$^+$ *uve1*::*LEU2*), EN3363 (*h*$^-$ *swi1-TAP*:*Kan*^{r}), EN3364 (*h*$^+$ *swi3*::*Kan*^{r}), EN3365 (*h*^{90} *swi3*::*Kan*^{r}), EN3366 (*h*$^-$ *swi3*::*Kan*^{r}), EN3367 (*h*^{90} *swi3-1*), EN3368 (*h*$^-$ *swi1-TAP*:*Kan*^{r} *swi3-13myc*:*Kan*^{r}), EN3369 (*h*$^-$ *swi3-13myc*:*Kan*^{r}), EN3370 (*h*$^-$ *swi3-TAP*:Kan^r *swi1-13myc*:*Kan*^{r}), EN3371 (*h*$^-$ *swi1-13myc*:*Kan*^{r}), EN3372 (*h*$^-$ *swi1*::*Kan*^{r} *swi3*::*Kan*^{r}), EN3373 (*h*$^-$ *swi3*::*Kan*^{r} *cds1*::*ura4*$^+$), EN3374 (*h*$^-$ *swi3*::*Kan*^{r} *chk1*::*ura4*$^+$), EN3375 (*swi3*::*Kan*^{r} *rad13*::*ura4*$^+$ *uve1*::*LEU2*), EN3376 (*h*$^-$ *rad22-YFP*:*Kan*^{r} *swi3*::*Kan*^{r}), EN3377 (*h*$^-$ *swi1-3FLAG*:*Kan*^{r} *cdc25-22*), EN3378 (*h*$^+$ *swi3-3FLAG*:*Kan*^{r} *cdc25-22*), EN3379 (*h*$^-$ *swi1-3FLAG*:*Kan*^{r} *swi3*::*Kan*^{r}), EN3380 (*h*$^-$ *swi3-3FLAG*:*Kan*^{r} *swi1*::*Kan*^{r}), EN3381 (*h*$^-$ *swi1-3FLAG*:*Kan*^{r}), EN3382 (*h*$^-$ *swi3-3FLAG*:*Kan*^{r}), EN3383 (*h*$^-$ *swi1-GFP*:*Kan*^{r} *swi3*::*Kan*^{r}), EN3384 (*h*$^+$ *swi3-GFP*:*Kan*^{r}), EN3385 (*h*$^-$ *swi3-GFP*:*Kan*^{r} *swi1*::*Kan*^{r}), EN3410 (*h*$^+$ *swi1*::*Kan*^{r}), EN3455 (*h*$^-$ *smt0 swi1*::*Kan*^{r} *rad22*::*ura4*$^+$), EN3456 (*h*$^-$ *smt0 swi3*::*Kan*^{r} *rad22*::*ura4*$^+$), EN3457 (*mus81*::*Kan*^{r} *rad22*::*ura4*$^+$), EN3458 (*swi1*::*Kan*^{r} *mus81*::*Kan*^{r} *rad22*::*ura4*$^+$), EN3459 (*swi1-*

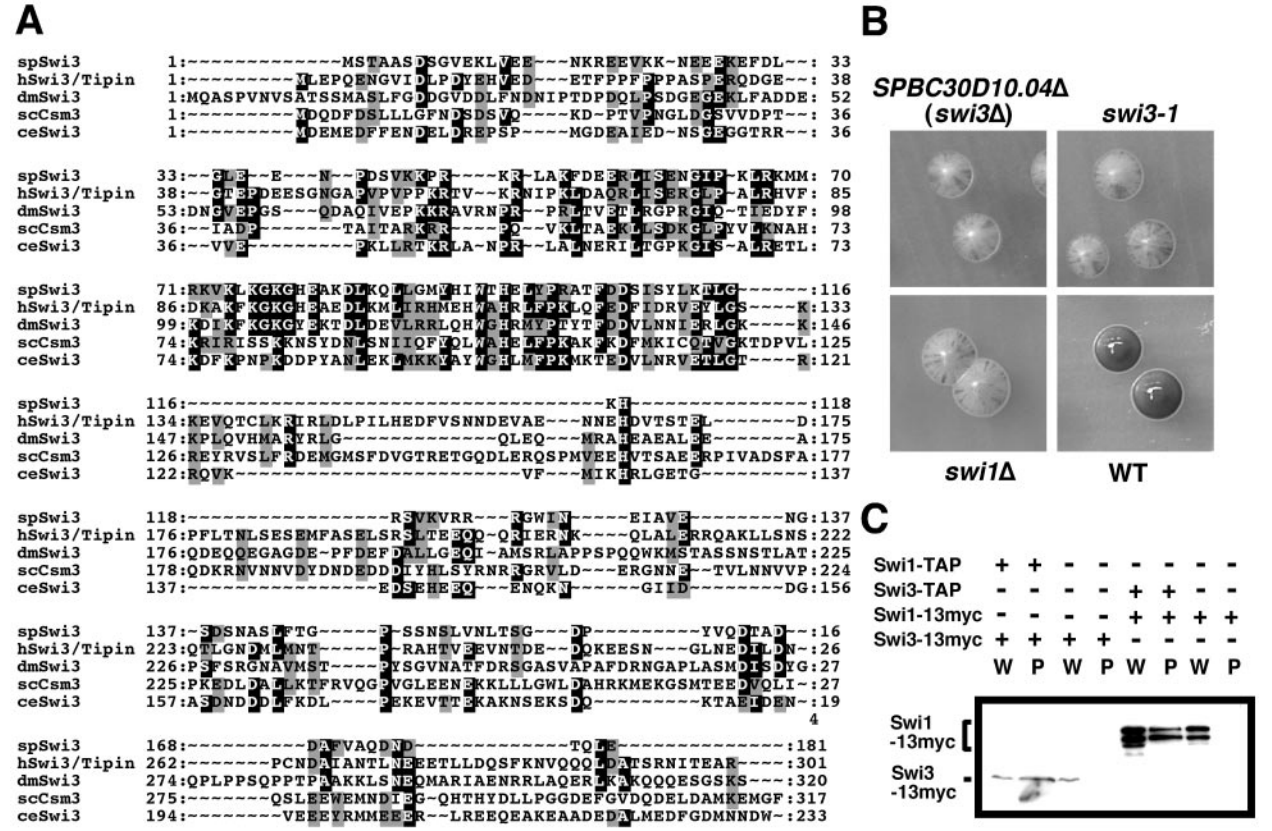

FIG. 1. Identification of Swi3 as a Swi1-interacting protein. (A) Swi3 is conserved across evolution. Multiple alignments of Swi3 homologs from *S. pombe* (spSwi3; GenBank accession no. AY498547), humans (hSwi3/Tipin; GenBank accession no. NP_060328), *Drosophila* (dmSwi3; GenBank accession no. NP_609895), *S. cerevisiae* (scCsm3), and *C. elegans* (ceSwi3; GenBank accession no. NP_490977) are shown. (B) Deletion of SPBC30D10.04 (*swi3*Δ), *swi3-1*, and *swi1*Δ showed inefficient mating-type switching. Homothallic h^{90} strains with the indicated genotypes were incubated on sporulation medium for 6 to 7 days at 25°C. Plates were exposed to iodine vapors. Colonies that have efficient mating-type switching stain darkly with iodine vapors, whereas inefficient strains show mottled staining. (C) Swi1 and Swi3 form a protein complex in *S. pombe*. Cells expressing Swi1 or Swi3 as TAP or 13myc fusion proteins were used for coimmunoprecipitation studies. TAP proteins were precipitated and probed with anti-myc antibodies. All proteins were expressed at endogenous levels. W, whole-cell extract; P, precipitated fraction.

13myc:*Kan*^{r} *rad11-3FLAG*:*Kan*^{r} *cdc25-22*), JL1307 (h^+ *cdc20-M10 ade6-210 his7-366*), KT2751 (h^- *cds1*::*ura4*$^+$), PR109 (h^-), PS2382 (h^- *smt0 rhp54*::*ura4*$^+$), PS2383 (h^- *smt0 rhp51*::*ura4*$^+$), PS2384 (h^- *smt0 rad22*::*ura4*$^+$), and PS2375 (h^- *rqh1*::*ura4*$^+$). All strains are *leu1-32* and *ura4-D18*.

RESULTS

Identification of the Swi1-Swi3 complex. We used MudPIT to identify proteins that associated with the Swi1-TAP fusion protein expressed at endogenous levels from the *swi1*$^+$ promoter. TAP consists of protein A and calmodulin binding domains separated by a tobacco etch virus protease cleavage site, allowing efficient two-step affinity purification of TAP-tagged proteins (50). MudPIT combines multidimensional liquid chromatography with electrospray ionization tandem mass spectrometry and proteomic methods to identify proteins in complex mixtures (65). The *swi1-TAP* strain used for these studies was not abnormally sensitive to genotoxic agents such as HU, indicating that Swi1-TAP was functional and retained physiologically significant protein interactions.

MudPIT analysis of Swi1-TAP identified Swi1 itself and a reproducible set of background proteins that are routinely identified in TAP fusion protein samples, together with a small number of potential interacting proteins. In the latter class, the highest coverage was of a predicted 148-amino-acid protein encoded by the SPBC30D10.04 open reading frame. Fourteen peptides from SPBC30D10.04 were identified. Sequence analysis of the corresponding cDNA revealed that this protein was actually derived from two exons that when spliced encoded a 181-amino-acid protein (Fig. 1A). This protein (which proved to be Swi3 [see the next paragraph]) has no evident protein motif, but it does have significant sequence similarity, especially between amino acids 38 and 116, to related proteins in budding yeast, humans, and other eukaryotes (Fig. 1A).

We were intrigued to find that SPBC30D10.04 is located between *spo6* and *ade1* on chromosome II in a region where *swi3* has been genetically mapped (2). We therefore investigated whether SPBC30D10.04 was allelic to *swi3*. We first examined mating-type switching efficiency. Mating-type switching within a single colony leads to mating and formation of spores that stain brown when exposed to iodine vapor. The strain with SPBC30D10.04Δ displayed a severe switching defect that was comparable to the defect in *swi1*Δ and *swi3-1* mutants (Fig. 1B). We then cloned the SPBC30D10.04 genes from wild-type and *swi3-1* strains and expressed them in the

swi3-1 mutant. Only the SPBC30D10.04 clone from the wild-type strain rescued the mating-type switching defect of *swi3-1* cells. Likewise, only the SPBC30D10.04 clone from the wild-type strain complemented the sensitivity that *swi3-1* cells displayed to the genotoxic drugs HU and camptothecin (CPT). Finally, we sequenced the SPBC30D10.04 clone from the *swi3-1* strain and found that it had an extra adenine at the 126th nucleotide. This mutation caused a frameshift that truncated the protein at amino acid 44. These results established that SPBC30D10.04 was allelic to *swi3*$^+$.

To confirm the interaction of Swi1 and Swi3 in *S. pombe*, the strain expressing Swi1-TAP was engineered to express Swi3-13myc from the *swi3* genomic locus. As expected, Swi3-13myc coprecipitated with Swi1-TAP (Fig. 1C). We also constructed a strain that expressed Swi3-TAP and Swi1-13myc from their own genomic loci and found that Swi1-13myc copurified with Swi3-TAP (Fig. 1C). The immunoblot signal of Swi1-13myc was much stronger than that of Swi3-13myc (Fig. 1C), but this difference probably reflected poor binding of Swi3-13myc to the blotting membrane. This conclusion is based on the microscopic analysis of Swi1-GFP and Swi3-GFP expressed from their respective genomic loci in live cells (see Fig. 4A, below). We measured the intensity of the GFP signals as described in Materials and Methods and found that the GFP signal value was 631 ± 81/pixel for Swi1-GFP and 640 ± 113/pixel for Swi3-GFP, indicating that both proteins were equally abundant in live cells (see Fig. 4A). Coupled with the evidence that *swi1* and *swi3* mutants present similar phenotypes in mating-type switching assays, these data strongly suggested that Swi1 and Swi3 function in a codependent manner as a stable heterodimer.

Swi3 is required for survival of fork arrest and for the replication checkpoint. We carried out a series of studies to determine whether Swi3 is involved in tolerance of fork arrest. These studies were modeled on previous investigations of Swi1 (41). We first investigated whether Swi3 contributed to survival of DNA lesions that block replication forks. For these studies we used UV irradiation. UV light creates cyclobutane dimers and other lesions that arrest replication forks. These studies were carried out in strains that were defective for nucleotide excision repair (*rad13*Δ) and UV damage excision repair (*uve1*Δ). Nucleotide excision repair and UV damage excision repair account for all detectable UV damage repair in fission yeast (69). Strains defective for both pathways are acutely sensitive to UV. Their UV survival depends on homologous recombination or translesion DNA polymerase pathways that bypass UV lesions during DNA replication (9, 18, 67). *swi3*Δ cells were not significantly sensitive to low doses of UV, but the *swi3*Δ mutation substantially enhanced UV sensitivity in the *rad13*Δ *uve1*Δ double mutant background (Fig. 2A), indicating that Swi3 is vital for viability when UV damage in DNA is not repaired.

We performed experiments to detect interactions between *swi3*Δ and mutations in checkpoint kinases in UV survival assays. The *chk1*Δ *swi3*Δ cells were substantially more sensitive than either single mutant (Fig. 2B). In contrast, there was no genetic interaction between *swi3*Δ and *cds1*Δ in UV survival assays. Chk1 is the effector kinase of the G_2-M DNA damage checkpoint. The interaction of *chk1*Δ and *swi3*Δ mutations in UV survival assays may be explained by one or a combination

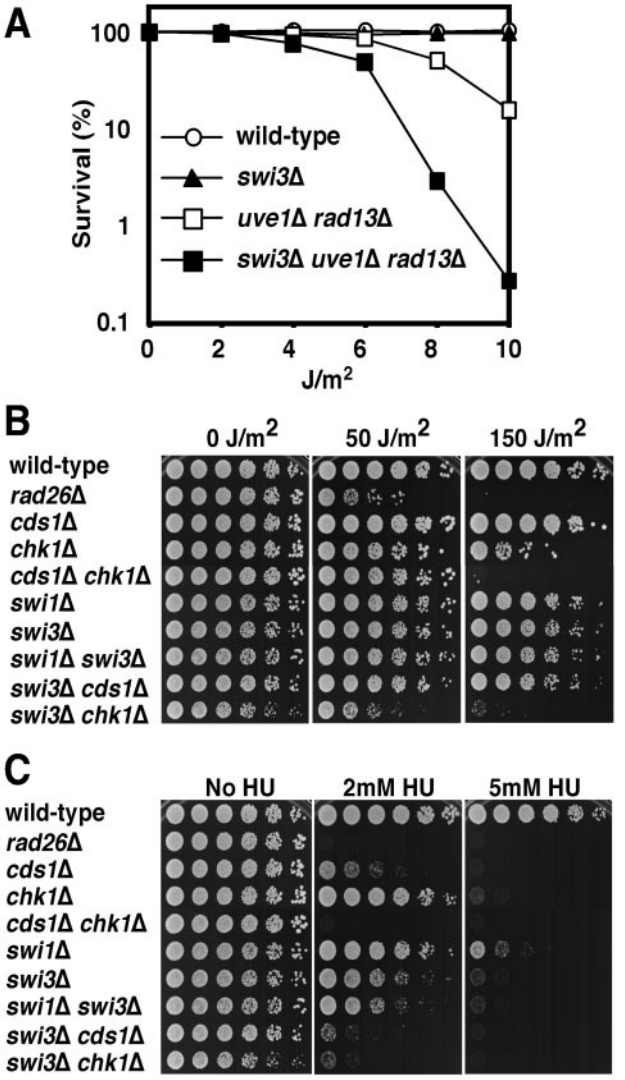

FIG. 2. Swi3 is required for survival of fork arrest. (A) Swi3 contributes to survival with UV irradiation in a *rad13*Δ *uve1*Δ strain that cannot excise UV damage. Cells of the indicated genotypes were spread on YES agar medium and exposed to the indicated dose of UV. Agar plates were incubated for 3 days at 30°C to measure UV survival. (B) Interaction of *swi3*Δ and *chk1*Δ mutations in UV survival assays indicates that Swi1 is required for tolerance of UV damage during DNA replication. Fivefold serial dilutions of cells were plated on YES agar medium and exposed to the indicated dose of UV. Agar plates were incubated for 2 to 5 days at 30°C. (C) Swi3 has a role in tolerating HU-induced fork arrest. *swi3*Δ cells were highly sensitive to HU. Synergistic interactions of *swi3*Δ with *cds1*Δ and *chk1*Δ mutations indicate that Swi3 has an HU survival function that is at least partially independent of Cds1 and Chk1. Fivefold serial dilutions of cells were incubated on YES agar medium supplemented with the indicated amounts of HU for 2 to 5 days at 30°C.

of two mechanisms. The *chk1*Δ mutation allows cells irradiated in G_2 phase to undergo mitosis and initiate a new round of DNA synthesis with unrepaired UV lesions. These lesions will obstruct replication forks and create an increased demand for Swi3's function in stabilizing stalled forks. In addition, the absence of Swi3 during S phase in cells containing UV lesions in DNA may lead to fork breakage or other abnormal DNA

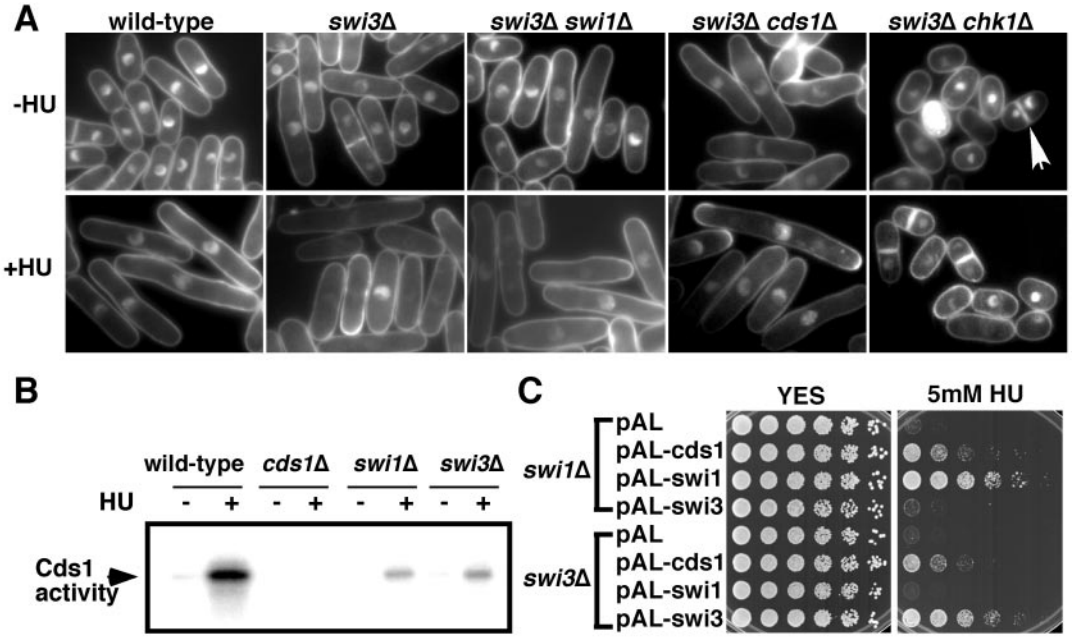

FIG. 3. Swi3 is required for the replication checkpoint. (A) Indicated strains were incubated in YES liquid medium supplemented with 0 or 12 mM HU for 6 h at 30°C and then stained with DAPI to visualize nuclear DNA as described in Materials and Methods. Wild-type, *swi3*Δ, *swi3*Δ *swi1*Δ, and *swi3*Δ *cds1*Δ cells treated with HU underwent checkpoint arrest, as indicated by the appearance of elongated, uninucleate cells without septa. In contrast, *swi3*Δ *chk1*Δ cells treated with HU failed to undergo cell cycle arrest and instead displayed aberrant mitosis, as indicated by a cut phenotype. The cut phenotype also appeared in ~10% of septated *swi3*Δ *chk1*Δ cells grown in the absence of HU (indicated by arrow). In some of the HU-treated cells the nuclei were not stained efficiently with DAPI. (B) Cds1 kinase activation is defective in *swi1*Δ and *swi3*Δ cells. Cells of the indicated genotypes were incubated in YES liquid medium supplemented with 0 or 12 mM HU for 4 h at 30°C. Kinase activity of immunoprecipitated Cds1 was measured by using myelin basic protein as a substrate. (C) HU sensitivity of *swi1*Δ or *swi3*Δ cells was suppressed by a multicopy *cds1*$^+$ plasmid. The *swi1*Δ or *swi3*Δ cells were transformed with the indicated plasmid and plated on YES medium containing 0 or 5 mM HU for 2 to 5 days at 30°C.

structures, creating an increased requirement for Chk1's function in the G_2-M checkpoint. In either case the data support the idea that Swi3 has an important role in tolerance of DNA damage caused by UV.

We also examined whether Swi3 is required to survive exposure to HU. *swi3*Δ cells displayed strong HU sensitivity (Fig. 2C). Interestingly, *swi3*Δ and *swi1*Δ *swi3*Δ cells were more HU sensitive than *swi1*Δ cells, indicating that, in addition to its functions in partnership with Swi1, Swi3 might have additional functions that are independent of Swi1 or that Swi3 retains a partial function in the absence of Swi1. There was an additive interaction between *swi3*Δ and *cds1*Δ (Fig. 2C), showing that Swi3 has a role in tolerating HU-induced replication arrest that is partially independent of Cds1.

To investigate Swi3's role in HU-induced checkpoint arrest, we examined the effect of inactivating Swi3 in *swi1*Δ, *cds1*Δ, and *chk1*Δ backgrounds. *swi3*Δ and *swi3*Δ *cds1*Δ cells arrested division (Fig. 3A), but *swi3*Δ *chk1*Δ cells failed to arrest (Fig. 3A). The latter observation was consistent with the strong interaction between *swi3*Δ and *chk1*Δ mutations in HU survival assays (Fig. 2C). Cds1 and Chk1 define redundant pathways of HU-induced checkpoint arrest (10); thus, the checkpoint defect of *swi3*Δ *chk1*Δ cells suggested that Swi3 is required for proficient function of Cds1. In support of this conclusion, Cds1 activation by HU was strongly diminished in *swi3*Δ cells (Fig. 3B). A similar deficiency in Cds1 activation was observed in *swi1*Δ cells (Fig. 3B).

In view of these findings, we examined whether the HU sensitivity of *swi1*Δ and *swi3*Δ cells could be rescued by overexpressing Cds1. This analysis showed that a multicopy plasmid that contained *cds1*$^+$ substantially rescued the HU sensitivity of *swi1*Δ and *swi3*Δ mutants (Fig. 3C). In contrast, Swi1 overexpression did not rescue the HU sensitivity of *swi3*Δ cells, nor did Swi3 overexpression rescue *swi1*Δ HU sensitivity (Fig. 3C).

The Swi1-Swi3 complex associates with chromatin in S phase. To determine whether the Swi1-Swi3 complex functions at replication forks and to further understand the functional relationship between Swi1 and Swi3, we investigated Swi1 and Swi3 localization by fluorescence microscopy using GFP-tagged proteins expressed from their endogenous promoters. Swi3-GFP-expressing cells were resistant to HU and CPT and proficient for mating-type switching, indicating that Swi3-GFP was fully functional. Swi3-GFP localized in the nuclei of all cells in an asynchronous culture, showing that Swi3 is nuclear throughout the cell cycle (Fig. 4A). After Triton X-100 extraction removed nuclear soluble proteins, Swi3-GFP persisted predominantly in septated cells and short cells (Fig. 4B). Septated cells are in S phase, and short cells are in late S or early G_2. Prior treatment with DNase I eliminated all Swi3-GFP (data not shown). Similar results were seen with the Swi1-GFP protein (41), indicating that the Swi1-Swi3 complex associates with chromatin only in S phase. These findings were consistent with the idea that the Swi1-Swi3 complex associates tightly with chromatin specifically during DNA replication.

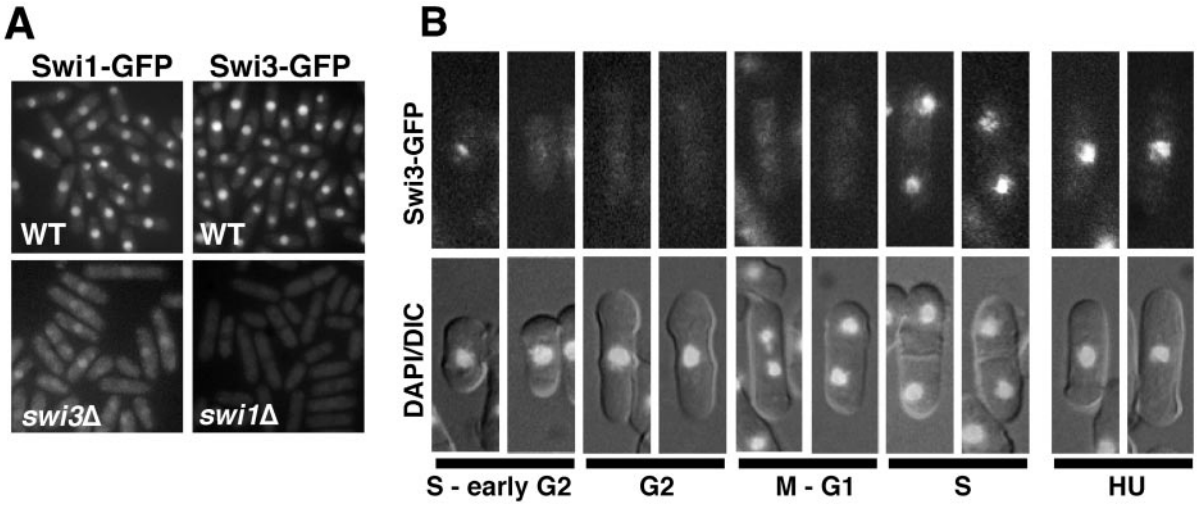

FIG. 4. Recruitment of Swi3-GFP to chromatin in S phase. (A) Swi1-GFP and Swi3-GFP are nuclear proteins. Swi1-GFP delocalized from the nucleus in *swi3*Δ cells. Swi3-GFP was not detectable in the absence of Swi1. Live cells were analyzed for Swi1-GFP or Swi3-GFP fluorescence. (B) In situ chromatin binding assay of Swi3-GFP. Spheroplasts were extracted with Triton X-100 to remove soluble nuclear protein and then fixed for microscopic analysis (41). Representative patterns of fluorescence are shown. Swi3-GFP was detected predominantly in septated cells and unseptated small cells, which are in S phase or possibly early G_2 phase. Representative photos of HU-treated cells are shown.

To further understand the functional relationship between Swi1 and Swi3, we examined Swi1-GFP localization in *swi3*Δ cells and Swi3-GFP localization in *swi1*Δ cells. Strikingly, the level of nuclear Swi1-GFP was strongly reduced in *swi3*Δ cells, and it was replaced by a strong cytoplasmic signal (Fig. 4A). The level of nuclear Swi3-GFP was strongly reduced in *swi1*Δ cells, but it was not replaced by an increase in the cytoplasmic signal of Swi3-GFP (Fig. 4A). Indeed, immunoblotting showed that Swi3 abundance was very low in *swi1*Δ cells (Fig. 5A), whereas Swi1 expression was unaffected in *swi3*Δ cells. The large reduction of Swi3 abundance in *swi1*Δ cells was curious in light of our studies showing that the phenotypes of *swi3*Δ cells were more severe than those seen in *swi1*Δ cells. These phenotypes suggested that residual amounts of Swi3 were present and presumably functional in *swi1*Δ cells. In fact, long exposures of the immunoblot showed that a small amount of Swi3 was detected in *swi1*Δ cells (Fig. 5A). These findings showed that Swi3's abundance in cells depends upon Swi1, and nuclear accumulation of Swi1 requires Swi3.

The Swi1-Swi3 complex moves with the replication fork. To address whether the S-phase-specific association of Swi1-Swi3 with chromatin reflects its localization at the replication fork, we performed ChIP with cells expressing FLAG- or myc-tagged proteins expressed from their endogenous promoters. The *cdc25-22* allele was used to synchronize cells at the G_2-M boundary. The *cdc25-22* strain was engineered to express both Swi1-13myc and Rad11-3FLAG proteins. Rad11 is the large subunit of the replication protein A (RPA) complex that binds ssDNA at the fork. We monitored Swi1-13myc at the *ars2004* replication origin and at two positions, 14 and 30 kb away from *ars2004* (42). Upon release from the arrest, Swi1-13myc associated with the replication origin *ars2004* at 60 min, and this association declined by 120 min (Fig. 5B). Swi1's association with *ars2004* occurred as the septation index increased, which coincided with the onset of S phase. Swi1's association with a site located 14 kb away from *ars2004* peaked at 60 to 100 min and declined by 140 min, shortly after its association with *ars2004*. Swi1's association with a site located 30 kb away from *ars2004* peaked slightly later, at 80 to 120 min, and declined by 160 to 180 min. The ChIP pattern of Rad11-3FLAG closely matched that of Swi1-13myc (Fig. 5B), suggesting that Swi1 associated with the moving replication fork. To further confirm that Swi1 relocates on chromatin during DNA replication, cells were released into the presence of a low dose of HU to extend the duration of S phase (Fig. 5C, upper panels). Peak association of Swi1 at *ars2004* occurred at 80 min and, thereafter, it slowly declined. The decrease in Swi1 at *ars2004* coincided with its increased association at the sites 14 and 30 kb away, again consistent with Swi1 moving with the fork. We obtained similar results with the Swi3-FLAG protein (Fig. 5C, bottom panels), suggesting that the Swi1-Swi3 complex moves with the fork.

Replication abnormalities in *swi3*Δ cells. Having established that Swi3 is required for tolerance of fork arrest and for checkpoint signaling to Cds1 and having found that it associates with chromatin in S phase, we then investigated Swi3's role in cells that have not been exposed to genotoxic agents. These studies were performed because several observations suggested that Swi3 was required for accurate DNA replication in the absence of genotoxic stress. In particular, we noticed that *swi3*Δ cells grown in the absence of genotoxic agents were moderately elongated in relation to wild type, whereas *swi3*Δ *chk1*Δ cells were not elongated (Fig. 3A). These phenotypes indicated that *swi3*Δ cells spontaneously accumulate unusual DNA structures that activate Chk1 and delay mitosis. Consistent with this possibility, we noted that *swi3*Δ *chk1*Δ cells frequently displayed a spontaneous "cut" phenotype. This phenotype was characterized by a DNA mass that was unequally distributed to daughter cells or bisected by the division plate (Fig. 3A). About 10% of the septated *swi3*Δ *chk1*Δ cells grown in liquid culture displayed a cut phenotype. Significantly, all of the *swi3*Δ *chk1*Δ phenotypes were also seen in *swi1*Δ *chk1*Δ cells but not in *cds1*Δ *chk1*Δ cells (41). The latter observation showed that the

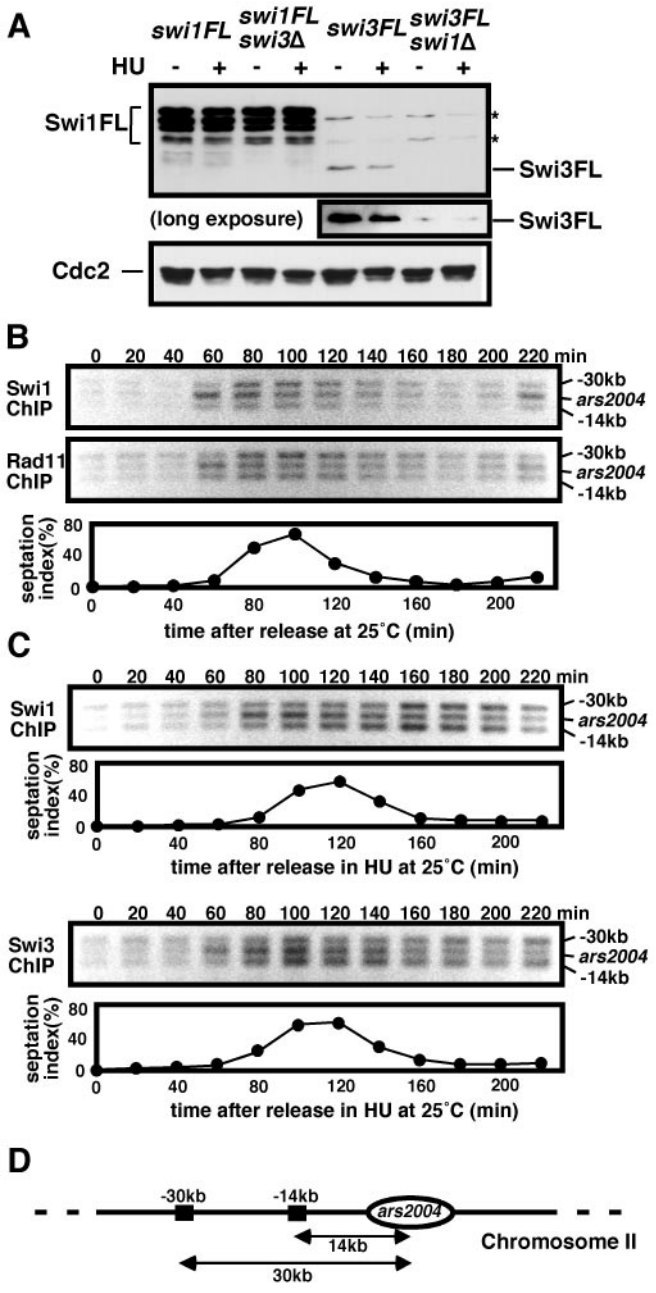

FIG. 5. Swi1 associates with the origin in early S phase. (A) Immunoblot analysis of Swi1-3FLAG (Swi1-FL) and Swi3-3FLAG (Swi3-FL). Cells of the indicated strains were incubated in YES medium supplemented with 0 or 12 mM HU. Protein samples of the indicated cells were analyzed by immunoblotting with anti-FLAG antibody. A longer exposure of the immunoblot showed that a very low amount of Swi3-FL was detected in *swi1*Δ cells. Asterisks show proteins that were cross-reactive with anti-FLAG antibody. (B) ChIP assays of Swi1-13myc and Rad11-3FLAG were performed at *ars2004* and sites located 14 or 30 kb away from *ars2004* (42). The *cdc25-22* cells were synchronized at the G_2-M boundary by incubation at 36°C for 4 h and then released in fresh YES medium at 25°C. An increase in the septation index indicates the onset of S phase. (C) ChIP assays of Swi1-FL and Swi3-FL were performed as described above, except that cells were released into YES medium supplemented with 10 mM HU. (D) Diagram of region used in the ChIP assay. *ars2004* and surrounding regions are shown.

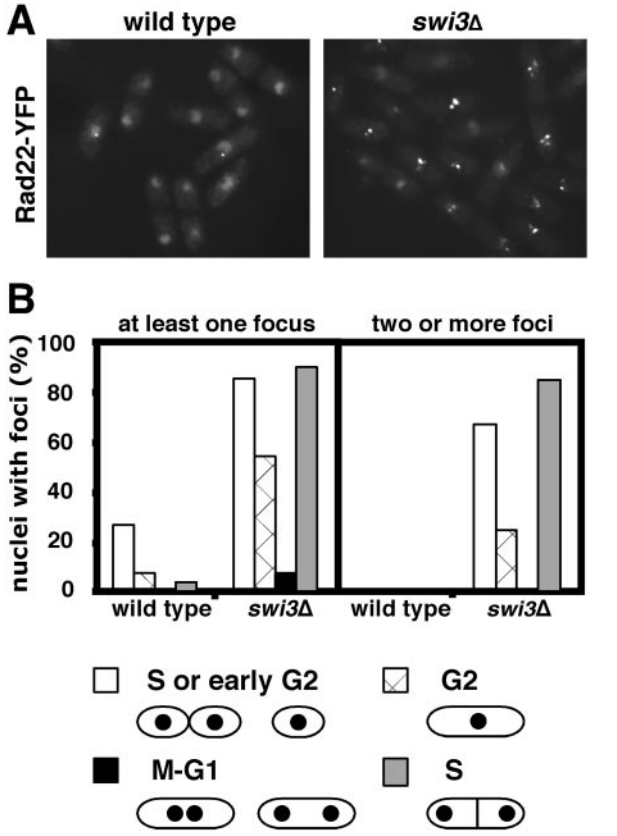

FIG. 6. Spontaneous DNA damage occurs during S phase in *swi3*Δ cells. (A) Multiple Rad22-YFP foci accumulated in *swi3*Δ cells. Log-phase cells were grown in Edinburgh minimal medium at 25°C. In wild-type cells, 15.8% of the nuclei contained a single Rad22-YFP focus and none showed multiple Rad22-YFP foci. In *swi3*Δ cells, 65.6% of the nuclei contained at least one Rad22-YFP focus and 48.9% had multiple foci. (B) Quantification of Rad22-YFP foci according to cell cycle stage estimated from cell and nuclear morphology. The percentages of nuclei that have at least one focus or two or more foci are shown. S-phase cells had the most Rad22-YFP foci.

genetic interactions involving *swi3*Δ and *chk1*Δ were not solely attributable to Swi3's role in Cds1 activation.

These findings suggested that *swi3*Δ cells suffer spontaneous DNA damage. This possibility was investigated further by monitoring the formation of Rad22 DNA repair foci in *swi3*Δ cells (15, 41). Fission yeast Rad22 (also known as Rad22A) is a homolog of budding yeast Rad52, a protein that binds to ssDNA during homologous recombination (47). If *swi3*Δ cells suffered broken forks or other forms of DNA damage as the result of replication abnormalities, these structures would be expected to recruit Rad22. Our studies were carried out with strains that expressed endogenous Rad22 tagged with yellow fluorescent protein (YFP). This analysis showed that there was a large increase in spontaneous Rad22-YFP foci in *swi3*Δ cells (Fig. 6A). In wild-type cells, 15.8% of nuclei contained a single Rad22-YFP focus and none showed multiple Rad22-YFP foci, whereas in *swi3*Δ cells 65.6% of the nuclei contained at least one Rad22-YFP focus and 48.9% had multiple foci (Fig. 6A).

We suspected that *swi3*Δ cells were suffering DNA damage or accumulating unusual DNA structures during DNA repli-

cation. This possibility was addressed by evaluating the cell cycle position of cells that contained Rad22-YFP foci. Cell cycle position in fission yeast can be estimated by noting cell length, nuclear morphology, and the appearance of a septum. S phase initiates very soon after nuclear division, continues during cell septation, and ends about when daughter cells finally detach. Cell cycle stage analysis revealed that *swi3*Δ cells with multiple Rad22-YFP foci were predominantly in S or early G_2 (Fig. 6B), indicating that the foci arose from DNA replication abnormalities. A similar phenotype was observed with *swi1*Δ cells (41), whereas *cds1*Δ cells displayed only a small increase in Rad22-YFP foci (41). These findings provided evidence that the Swi1-Swi3 complex has Cds1-independent functions that help ensure faithful DNA replication.

Rhp51 and Rhp54 are not required for survival of *swi3*Δ *cells*. Rad52 homologs have well-established roles in double-strand break (DSB) repair (47). We therefore hypothesized that the increased Rad22-YFP foci in *swi3*Δ cells were representative of DSBs created by fork collapse. A broken fork produces a DNA free end that is resected on one strand as a prelude to repair by homologous recombination (Fig. 7A). Recapture of broken forks is thought to proceed by strand invasion and DNA annealing steps that are dependent on Rad51 and Rad54 (36, 47). This process is thought to necessarily lead to formation of an HJ (Fig. 7A). Current evidence in fission yeast indicates that Rhp51 and Rhp54 are needed for strand invasion of DNA duplexes, while the Mus81-Eme1 complex is required for HJ resolution (8, 19, 45). Consistent with the fork recapture model, Rhp51, Rhp54, and Mus81-Eme1 are required for survival of fork breakage caused by CPT, a topoisomerase I inhibitor (14).

To address whether *swi1*Δ and *swi3*Δ cells experience spontaneous fork breakage, we carried out genetic crosses that introduced *swi1*Δ or *swi3*Δ mutations into *rhp51*Δ or *rhp54*Δ strains. Tetrad analysis revealed that *rhp51*Δ and *rhp54*Δ mutations displayed no obvious genetic interactions with *swi1*Δ or *swi3*Δ mutations (Table 1). Viable double mutants were recovered at the expected frequency, and they grew as well as the *rhp51*Δ and *rhp54*Δ single mutants. Given the vital role that Rhp51 and Rhp54 play in homologous recombination and survival of CPT treatment (14), these findings strongly indicated that *swi1*Δ and *swi3*Δ strains do not experience an elevated occurrence of fork breakage.

We also performed a genetic cross involving *swi3*Δ and *mus81*Δ mutations. In contrast to the situation with *rhp51*Δ and *rhp54*Δ mutations, *swi3*Δ had a synthetic lethal interaction with *mus81*Δ (Table 1). The *swi3*Δ *mus81*Δ spores germinated and formed microcolonies of ~4 to 30 elongated or misshapen cells. No viable *swi3*Δ *mus81*Δ cells were recovered among 33 double mutant spores. A very similar genetic interaction was seen with *swi1*Δ and *mus81*Δ mutations (41). Tetrad analysis revealed that 35 of 37 *swi1*Δ *mus81*Δ spores germinated to produce inviable microcolonies. The other two *swi1*Δ *mus81*Δ spores propagated to form very slow growing colonies that contained many dead cells. Taken together, these studies provided strong evidence that *swi1*Δ and *swi3*Δ strains experience replication abnormalities that lead to HJ formation without fork breakage.

X-shaped DNA structures accumulate in *swi1*Δ *mus81*Δ *cells*. The genetic interactions described above suggested that *swi1*Δ and *swi3*Δ mutants form abnormal DNA structures during DNA replication that recombine to form HJs by an Rhp51- and Rhp54-independent mechanism. We explored this possibility by performing 2D gel electrophoresis of chromosomal DNA to detect branched DNA structures. X-shaped DNA migrates in a characteristic spike in 2D gels (Fig. 7D). We monitored the *ars3001* HindIII-KpnI region. This region contains the replication origin of the rDNA (41, 51). We analyzed wild-type, *mus81*Δ, *swi1*Δ, *swi3*Δ, and *cds1*Δ strains, as well as *cds1*Δ *mus81*Δ and *swi1*Δ *mus81*Δ double mutants (Fig. 7B). The latter strain was derived from one of the very slow growing *swi1*Δ *mus81*Δ strains mentioned above. The amount of X-shaped DNA was quantified as the percentage of replication and recombination intermediates (Fig. 7B). Wild-type, *swi1*Δ, *swi3*Δ, and *cds1*Δ strains contained approximately equal amounts of X-shaped DNA (14.2 to 19.6%, expressed as a percentage of the total replication and recombination intermediates), whereas X-shaped DNA was increased in the *mus81*Δ cells (26.7%). Importantly, there was substantially more X-shaped DNA in *swi1*Δ *mus81*Δ cells (38.6%). In contrast, the amount of X-shaped DNA in *cds1*Δ *mus81*Δ cells (29.1%) was not substantially increased relative to that in *mus81*Δ cells (Fig. 7B).

The structure of the X-shaped DNA in *swi1*Δ *mus81*Δ cells was investigated further by performing branch migration assays (6, 19, 53, 70). In these assays HJs branch migrate to form linear DNA fragments. The agarose gel slice from the first-dimension gel electrophoresis was incubated in branch migration buffer at 65°C for 5 h prior to 2D gel electrophoresis (Fig. 7C). A control gel slice was incubated at 4°C for 5 h. When incubated at 65°C, the amount of X-shaped DNA in *swi1*Δ *mus81*Δ cells was strongly reduced (Fig. 7C and D). The branch migration reaction produced a distinct spot that migrated directly below the X-shaped DNA at the level of linear fragment (Fig. 7C and D), indicating that the majority of X-shaped DNAs in *swi1*Δ *mus81*Δ cells were HJs, or possibly hemicatenanes that formed by the fusion of HJs (32, 66).

Rad22 inactivation suppresses *swi1*Δ *mus81*Δ synthetic lethality and formation of X-shaped DNA. The aforementioned studies suggested that the absence of functional Swi1-Swi3 complex leads to the formation of ssDNA regions that are bound by Rad22 and are converted into HJs. If there was a causal connection between formation of Rad22 foci and the appearance of HJs in *swi1*Δ *mus81*Δ cells, we would expect that inactivation of Rad22 might ameliorate the genetic interactions involving *swi1*Δ and *mus81*Δ. Moreover, if HJs were formed without the participation of Rhp51 and Rhp54, as suggested by our studies, it would be expected that inactivation of Rhp51 and Rhp54 should not rescue the synthetic lethal interactions involving *swi1*Δ and *mus81*Δ. Indeed, genetic crosses showed that *rhp51*Δ and *rhp54*Δ mutations did not suppress *swi1*Δ *mus81*Δ synthetic lethality (Table 1). In contrast, *swi1*Δ *mus81*Δ *rad22*Δ cells were viable, although they grew slowly relative to each of the single mutants (Table 1).

These results suggested that the Rad22 foci detected in *swi1*Δ and *swi3*Δ mutants were precursors of HJs that were formed, apparently without fork breakage, in a reaction requiring DNA strand annealing promoted by Rad22. To test this possibility, we examined whether the increase in X-shaped DNA in *swi1*Δ *mus81*Δ cells required Rad22. The amount of

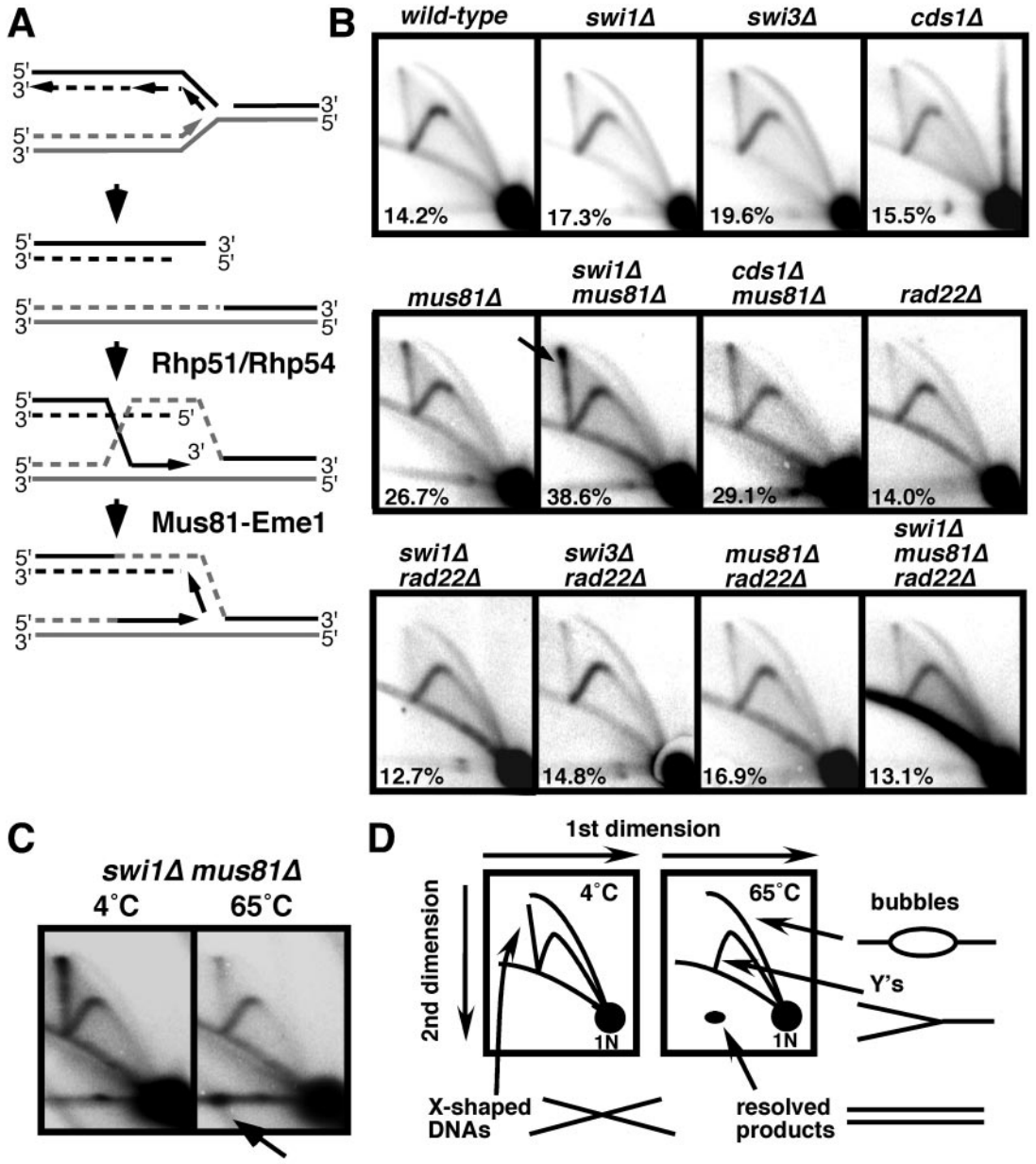

FIG. 7. *swi1*Δ cells accumulate X-shaped DNA. (A) Model of the fork recapture mechanism. Fork recapture requires strand invasion catalyzed by Rhp51 and Rhp54 followed by HJ resolution by the Mus81-Eme1 complex. (B) X-shaped DNA accumulates in *swi1*Δ *mus81*Δ cells. Genomic DNA samples prepared from exponentially growing *S. pombe* cells with the indicated genotypes were analyzed by 2D gel electrophoresis with the *ars3001* HindIII-KpnI fragment as a probe (41). The amount of X-shaped DNA expressed as the percentage of entire replication and recombination intermediates was quantified. The arrow points to X-shaped DNA in *swi1*Δ *mus81*Δ cells. (C) The X-shaped DNA branch migrates into linear DNA. Genomic DNA from *swi1*Δ *mus81*Δ cells was run in the first-dimension gel and gel slices were incubated in branch migration buffer at 4 or 65°C for 5 h, as described in Materials and Methods, and then DNA was electrophoresed in the 2D gel. The arrow indicates the spot corresponding to the linear DNA products derived from the X-shaped DNA molecules by branch migration. (D) Diagram of the migration pattern of replication and recombination intermediates that can be detected by 2D gel electrophoresis before (4°C) and after (65°C) the branch migration reaction. X-shaped DNA that has the property of HJs can be converted into a linear product that produces a distinct spot which migrates below the X-shaped DNA on the 1N line.

X-shaped DNA in *swi1*Δ *mus81*Δ *rad22*Δ cells (13.1%) was approximately equivalent to that seen in *swi1*Δ (17.3%) and *rad22*Δ (14.0%) single mutants (Fig. 7B). These data suggested that accumulated ssDNA in the *swi1*Δ and *swi3*Δ mutants recombined to form HJs through a Rad22-dependent mechanism.

Interestingly, the amount of X-shaped DNA in *rad22*Δ cells and the wild type was approximately the same (Fig. 7B). The

TABLE 1. Genetic interactions involving *swi1*Δ and *swi3*Δ

Genotype	Growth rate[a]
Wild type	++++
*swi1*Δ	+++
*swi3*Δ	+++
*rhp51*Δ	++
*rhp54*Δ	++
*rad22*Δ	++
*mus81*Δ	++
*swi1*Δ *rhp51*Δ	++
*swi3*Δ *rhp51*Δ	++
*swi1*Δ *rhp54*Δ	++
*swi3*Δ *rhp54*Δ	++
*swi1*Δ *rad22*Δ	++
*swi3*Δ *rad22*Δ	++
*swi1*Δ *mus81*Δ	−[b]
*swi3*Δ *mus81*Δ	−[c]
*swi1*Δ *mus81*Δ *rhp51*Δ	−
*swi1*Δ *mus81*Δ *rhp54*Δ	−
*swi1*Δ *mus81*Δ *rad22*Δ	+

[a] Doubling times: ++++, ~2 h; +++, ~2.5 h; ++, ~3 h; +, ~6 h; −, no growth.
[b] Two out of 37 *swi1*Δ *mus81*Δ spores were viable.
[c] None of the 33 *swi3*Δ *mus81*Δ spores was viable.

presence of this Rad22-independent X-shaped DNA seems to contradict earlier studies in *S. pombe* and *S. cerevisiae* (53, 70), in which formation of X-shaped DNA required Rad22/Rad52. However, recent studies of *S. cerevisiae* have shown that X-shaped DNA can form without Rad52 (32, 66). These studies used a modified method of preparing DNA that preserves X-shaped DNA structures. In this study, we have detected both Rad22-dependent and -independent X-shaped DNA. We suspect that the Rad22-dependent X-shaped DNA molecules are HJs, because they arose in the *mus81*Δ background and readily branch migrated. The Rad22-independent X-shaped DNA might be converged forks or hemicatenanes.

Specific genetic interactions involving the Swi1-Swi3 complex and DNA polymerases. Previous studies showed that Swi1 and Swi3 are required for viability in a strain that has the *swi7-1* (DNA polymerase α [Polα]) mutation that impairs mating-type switching (52). Polα is required to initiate both leading- and lagging-strand synthesis (63). To further explore the source of the abnormal DNA structures in *swi1*Δ and *swi3*Δ cells, we examined genetic interactions with *cdc6-23* (Polδ) and *cdc20-M10* (Polε) mutations. The exact roles of these polymerases are uncertain, but mutational analyses using exonuclease-deficient Polδ and Polε strains have shown a strand specificity of mutation rates and spectra, suggesting that the two polymerases operate preferentially on different sides of the fork (24, 48, 54). We found that *swi1*Δ and *swi3*Δ mutations were synthetically lethal with *cdc6-23* but not with *cdc20-M10*. We cannot exclude the possibility that *swi1*Δ and *swi3*Δ might have genetic interactions with other alleles of *cdc20*, but the specific genetic interactions with DNA Polα and Polδ suggest that Swi1-Swi3 might be required to coordinate leading- and lagging-strand synthesis.

DISCUSSION

We have shown that Swi1 and Swi3 function together in a protein complex that helps to maintain genome integrity in fission yeast. This complex is recruited to chromatin in S phase, and it travels in close proximity to the replication fork. It is needed to pause the replication fork at specific sites near the *mat1* locus, and it is required for proficient activation of the replication checkpoint in response to fork arrest. In the absence of the Swi1-Swi3 complex, abnormal DNA structures represented by Rad22 foci accumulate during S phase. These structures are unlikely to be broken forks, because *rhp51*Δ and *rhp54*Δ do not have genetic interactions with *swi1*Δ and *swi3*Δ mutations. Instead, we hypothesize that the Rad22 foci represent ssDNA gaps that can mature into HJs or related structures that are processed by Mus81-Eme1 resolvase. Both *swi1*Δ and *swi3*Δ have striking genetic interactions with mutations that impair DNA Polα and Polδ but not Polε. In view of these and earlier studies, we suggest that the Swi1-Swi3 heterodimer can be described as an FPC that is required to properly coordinate leading- and lagging-strand synthesis. We suggest that an inability to coordinate leading- and lagging-strand synthesis in FPC-deficient cells leads to formation of ssDNA gaps during S phase, as well as an inability to activate the replication checkpoint.

Swi1-Swi3 FPC. Swi1 and Swi3 readily coprecipitate as components of a stable complex. We cannot formally exclude the possibility that there may be other proteins in this complex, but mass spectrometry and genetic studies have failed to identify additional candidates. In cells that express GFP-tagged Swi1 or Swi3 from the endogenous loci, the two proteins appear to be expressed at a 1:1 ratio and they colocalize in the nucleus. Swi3 appears to be very unstable in *swi1*Δ cells, whereas Swi1 is delocalized from the nucleus in *swi3*Δ cells. The *swi1*Δ and *swi3*Δ mutations impart nearly identical phenotypes in a wide range of assays, with the only exception being that *swi3*Δ cells appear to be slightly more sensitive to HU. Taken together, these data show that Swi1 and Swi3 function as an integrated, self-contained complex.

Our studies suggest that the Swi1-Swi3 FPC is closely associated with the replication fork, and it may in fact be an ancillary component of the larger replisome complex. FPC associates with chromatin specifically in S phase, and it moves away from a replication origin in synchrony with RPA. These findings are consistent with genome-wide studies of *S. cerevisiae* Tof1, the presumptive homolog of Swi1 (25). Exactly how FPC associates with the fork is unknown. Tof1 was shown to coprecipitate with the essential DNA replication protein Cdc45 specifically during S phase (25); thus, it is reasonable to speculate that Cdc45 (Sna41 in fission yeast) or an associated protein recruits FPC to replication forks. In such a position, FPC is well placed to stabilize stalled forks in a configuration that can be recognized by the replication checkpoint system.

Abnormal DNA structures in FPC mutants. Genetic interactions involving *swi1*Δ and *swi3*Δ mutations with *chk1*Δ strongly suggest that FPC mutants accumulate abnormal DNA structures during S phase that activate the DNA damage checkpoint. Deciphering the nature of this damage and FPC's role in DNA replication necessitates an understanding of homologous recombination repair. Rad51, Rad52, and Rad54 homologs play central roles in mediating strand invasion of resected DSBs into intact duplex targets (47). They are thought to perform the same activities in recapture of broken forks. In the case of fork recapture, strand invasion necessarily leads to

formation of a D-loop and an HJ or an HJ-like structure that must be resolved to allow chromosome segregation during mitosis (36). The Mus81-Eme1 complex is thought to resolve these structures (8, 19, 45). Consistent with these models, Rhp51, Rhp54, and Mus81-Eme1 endonuclease are all vital for survival of cells treated with CPT, a topoisomerase inhibitor that induces fork breakage (14). In contrast to the situation with CPT, Rhp51 and Rhp54 but not Mus81-Eme1 are required for survival of DSBs caused by ionizing radiation (9). These results suggest that DSBs in G_2 phase are preferentially repaired by synthesis-dependent strand annealing or a related mechanism (47) that requires strand invasion but not HJ resolution. Consistent with this notion, crossing over is rarely associated with mitotic recombination in *S. pombe* (62). Thus, synthesis-dependent strand annealing appears to be the dominant recombination mechanism of repairing DSBs in mitotic *S. pombe* cells, as it is in *S. cerevisiae* (47).

Mus81-Eme1, Rhp51, and Rhp54 are all required to survive CPT-induced fork breakage, whereas only Rhp51 and Rhp54 are required to survive DSBs caused by ionizing radiation. In *swi1*Δ and *swi3*Δ mutants, a third situation exists in which Mus81-Eme1, but not Rhp51 and Rhp54, is required for viability. These relationships imply that *swi1*Δ *mus81*Δ and *swi3*Δ *mus81*Δ cells form HJs without breaking forks. The alternative possibility is that FPC mutants suffer broken forks that are recaptured by a mechanism that does not require Rhp51 and Rhp54. It is conceivable that in some instances broken forks might be repaired without Rhp51 and Rhp54, for example, in the rDNA repeats. However, if broken forks were constrained to the rDNA, we would not expect to see multiple Rad22 foci in FPC mutants. We therefore conclude that Rad22 foci detected in *swi1*Δ and *swi3*Δ mutants are unlikely to represent broken forks and, thus, are probably sites of ssDNA gaps left in the wake of a moving replication fork. The idea that FPC mutants were not suffering broken forks was further strengthened by the fact that the *swi1*Δ *rad22*Δ *rhp51*Δ triple mutant was still highly viable (data not shown). A causal connection between Rad22 foci and Rad22-dependent formation of X-shaped DNAs is strongly suggested by the rescue of *swi1*Δ *mus81*Δ by *rad22*Δ. These genetic interactions indicate that a Rhp51/Rhp54-independent strand annealing activity of Rad22 promotes formation of recombination structures in *swi1*Δ and *swi3*Δ cells that must be resolved by Mus81-Eme1. Such a Rad51/Rad54-independent activity has been described for Rad52 in budding yeast (47). This activity of Rad22 is not required for viability in FPC mutants (Table 1); thus, it is likely that the ssDNA gaps in *rad22*Δ *swi1*Δ *mus81*Δ cells are repaired by a gap-filling mechanism similar to that involved in nucleotide excision repair.

Two models that illustrate how HJs might arise without fork breakage from a single-strand gap in the vicinity of a replication fork are shown in Fig. 8. These ssDNA gaps occur in the absence of FPC. These gaps may be generated when leading- and lagging-strand DNA synthesis are uncoordinated (see next paragraph). In model A, an ssDNA gap left in the wake of a replication fork becomes involved in strand exchange events that are promoted by Rad22. Coupled DNA synthesis leads to formation of double HJs that are cleaved by Mus81-Eme1. In principle, Mus81-Eme1 could cleave HJs or HJ precursors. We did not observe an increased amount of X-shaped DNA in *swi1*Δ or *swi3*Δ single mutants, suggesting that the HJs or HJ precursors can be readily resolved by Mus81-Eme1. An alternative possibility for formation of HJs without fork breakage is shown in Fig. 8B. In this model, problems with DNA synthesis in FPC mutants lead to fork regression and formation of a "chicken foot" structure that is similar to an HJ. The exposed nascent strand of DNA is bound by Rad22, which in turn promotes annealing to the template parental strand ahead of the fork. The activity of a replicative helicase might disassociate the parental strands ahead of the fork and thereby facilitate Rad22-dependent strand invasion.

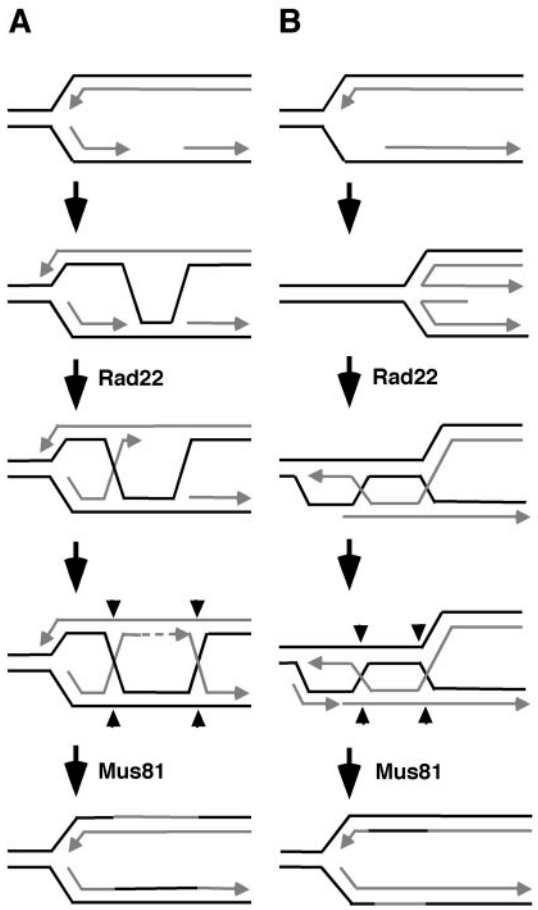

FIG. 8. Two models for Rad22-dependent generation of X-shaped DNA molecules and their resolution by Mus81-Eme1 in *swi1*Δ and *swi3*Δ cells. (A) The ssDNA gap left in the lagging strand participates in a recombination event catalyzed by Rad22. Strand invasion by the 3′ end of an Okazaki fragment and following DNA synthesis leads to formation of double HJs that are targeted by Mus81-Eme1. (B) An ssDNA gap may lead to fork regression, creating a chicken foot structure that is similar to an HJ. The exposed nascent strand of DNA may anneal to the template parental strand ahead of the fork, resulting in formation of double HJs.

Relationship between FPC and DNA Pols. The relationships involving *swi1*Δ and *swi3*Δ with *rhp51*Δ, *rhp54*Δ, and *mus81*Δ are not completely unique. Mutations in *swi7-1* (Polα) and *cdc6-23* (Polδ) also display strong genetic interactions with *mus81*Δ but not with *rhp51*Δ or *rhp54*Δ (9). Polα is required for both lagging- and leading-strand synthesis, while Polδ and Polε are thought to operate on different sides of the fork. Using the

same rationale described above, these genetic relationships suggest that *swi7-1* and *cdc6-23* mutants accumulate ssDNA gaps but not broken forks during S phase. One possible interpretation of these findings is that FPC works together with Polα and Polδ to promote effective DNA synthesis. This possibility is consistent with the synthetic lethal interactions involving *swi1*Δ and *swi3*Δ with *swi7-1* and *cdc6-23* mutations. Significantly, *swi1*Δ and *swi3*Δ did not display a synthetic lethal interaction with the *cdc20-M10* mutation that encodes a defective form of Polε. In this context, it is worth noting the correlations of our investigations with earlier studies by Zou and Rothstein (70). Working with budding yeast, they showed that Polα and Polδ mutations, but not Polε mutations, led to formation of X-shaped DNAs in the rDNA repeats by a mechanism that required Rad52 but not Rad51 or Rad54.

Genetic studies have indicated that Polδ and Polε operate on different DNA strands (24, 48, 54), and in one study it was further suggested that Polδ might be specifically involved in lagging-strand synthesis, although definitive evidence is lacking. On the basis of these studies and our evidence that the Swi1-Swi3 complex is essential in cells that are partially defective for Polδ but not Polε, it is tempting to speculate that Swi1-Swi3 FPC is needed to stabilize forks when lagging-strand synthesis is blocked. FPC might directly participate in lagging-strand synthesis, or it might be required to slow down the fork when lagging-strand replication encounters difficulties. Vengrova and Dalgaard recently made a similar suggestion (61). These difficulties could be in the form of DNA damage that blocks lagging-strand synthesis. Tof1, the Swi1 homolog in budding yeast, is required to retard replisome movement when DNA synthesis is inhibited by HU (25). Perhaps Tof1 and Swi1 are subunits of a molecular brake that slows down or arrests the replisome when dNTPs are unavailable or when lagging-strand synthesis encounters barriers.

FPC's checkpoint function. Swi1 and Swi3 have the properties expected of proteins that are specifically involved in the replication checkpoint. They are necessary for survival of genotoxic agents that arrest replication forks, they are required for HU-induced cell cycle arrest in a *chk1*Δ strain, and they are needed for proficient activation of Cds1. Moreover, the HU-sensitive phenotype of FPC mutants can be substantially rescued by overexpression of Cds1. Swi1 and Swi3 are not needed for the Chk1-dependent HU arrest that occurs in *cds1*Δ cells; thus, FPC is not required for Chk1 function. These findings show that FPC is specifically required for the replication checkpoint. The replication checkpoint properties of FPC closely match those of Mrc1, a protein that channels the replication checkpoint signal to Cds1 (1, 57). This specificity correlates with the fact that Mrc1 abundance is highly cyclical and specific for S phase (57) and with the observations that Swi1 and Swi3 associate with chromatin only in S phase.

While FPC, Mrc1, and Cds1 are all specifically required for the replication checkpoint, it is evident that *swi1*Δ and *swi3*Δ mutants differ from *cds1*Δ and *mrc1*Δ mutants. The mutations in *cds1*Δ and *mrc1*Δ do not impair mating-type switching, and they do not cause an increased incidence of aberrant mitosis in a *chk1*Δ background (41, 57). Inactivation of Cds1 causes only a small increase in Rad22 foci, and *cds1*Δ is not synthetic lethal with *mus81*Δ (9, 41). Unlike a number of DNA replication proteins that have been implicated in checkpoint signaling, FPC is not essential for DNA replication. Thus, the replication checkpoint defects in *swi1*Δ and *swi3*Δ cells cannot be readily ascribed to deficiencies in origin activation or DNA synthesis. These observations led us to conclude that FPC has a checkpoint-independent role in preserving replication forks, and this function stabilizes forks in a configuration that is required for efficient activation of the replication checkpoint kinase Cds1. These properties distinguish the Swi1-Swi3 FPC from previously described checkpoint proteins.

We previously showed that Swi1 associates with chromatin in S phase in a manner that is independent of other checkpoint proteins, such as Rad26, indicating that Swi1 has a role in DNA replication and checkpoint control that is independent of checkpoint activation (41). These finding suggested that FPC might be a component of a replisome whose primary role is to stabilize forks when they encounter obstacles. In this study, we showed that Swi1, as well as RPA, preferentially associates with a replication origin early in S phase and then associates with sites distal to the origin as replication proceeds. These findings suggest that Swi1 moves with the replication fork, consistent with recent studies of Tof1 (25). On the basis of these studies we propose that the Swi1-Swi3 complex moves with the fork and stabilizes it when it encounters a replication obstacle. In this model, FPC acts at a very early stage of fork stabilization and checkpoint signaling, whereas Cds1 acts at a later stage and is needed to maintain stalled replication forks in a stable state. Mrc1 might act as a bridge between the initial fork stabilization by FPC and maintenance of the stalled replication fork by Cds1.

FPC in other organisms. Is FPC conserved in other eukaryotes? As discussed above, Swi1 and Tof1 are structurally related and share a number of phenotypes and activities, and thus they are likely to be true functional homologs. There are some significant phenotypic differences between *swi1*Δ and *tof1*Δ cells, for example, *tof1*Δ cells are not sensitive to HU (17), but these differences probably reflect organism differences in repair and checkpoint systems as opposed to differences in Swi1 and Tof1 functions. Interestingly, a large-scale yeast two-hybrid screen identified a putative interaction between budding yeast Tof1 and the Swi3-related protein Csm3 (59), suggesting conservation of FPC in the two highly divergent yeasts. The Tof1-Csm3 interaction was recently confirmed by coimmunoprecipitation (35). Budding yeast *csm3*Δ mutants appear to have a mild defect in meiotic chromosome segregation (49), and recent studies have uncovered a partial sister chromatid cohesion defect in *tof1*Δ and *csm3*Δ cells (35, 64). This phenotype is interesting in light of the role of *C. elegans* Tim1 (Tof1/Swi1 homolog) in chromosome cohesion and segregation (12). *C. elegans* has a Csm3/Swi3 homolog (Fig. 1A), and we speculate that it functions together with Tim1. There may be a causal connection between fork protection and chromosome cohesion. FPC-dependent fork protection may assist in establishing cohesion during S phase. Another possibility is that FPC-dependent activation of Cds1 homologs may be involved in establishing chromosome cohesion. This proposal is consistent with evidence that a mutation in *C. elegans chk-2*, a *cds1* homolog, causes defects in meiotic chromosome segregation (34).

Drosophila and mammalian Timeless (Tim1) have been characterized as proteins that regulate circadian rhythms (5).

At present we cannot offer a model that connects circadian rhythm control to fork protection, checkpoint signaling, or chromosome cohesion. However, a mouse Csm3/Swi3 homolog named TIPIN was recently detected in a two-hybrid screen with mouse Tim1 (20). Thus, it appears that the protein complexes related to Swi1-Swi3 and Tof1-Csm3 are broadly conserved among eukaryotes. It will be interesting to determine whether these complexes are involved in DNA replication and maintenance of genome integrity.

ACKNOWLEDGMENTS

We thank V. Martin for providing the Rad11-3FLAG strain. Members of the Scripps Cell Cycle groups are thanked for their support and encouragement. We thank Joel Huberman for his helpful discussion.

E.N. was a fellow of the Human Frontier Science Program. E.N. was also supported by the UEHARA Memorial Foundation. This work was funded by MERK-MGRI-241 (W.H.M. and J.R.Y.), NIH EY1328801 (J.R.Y.), and NIH grant GM59447 awarded to P.R.

REFERENCES

1. **Alcasabas, A. A., A. J. Osborn, J. Bachant, F. Hu, P. J. Werler, K. Bousset, K. Furuya, J. F. Diffley, A. M. Carr, and S. J. Elledge.** 2001. Mrc1 transduces signals of DNA replication stress to activate Rad53. Nat. Cell Biol. **3:**958–965.
2. **Alfa, C., P. Fantes, J. Hyams, M. McLeod, and E. Warbrick.** 1993. Experiments with fission yeast. Cold Spring Harbor Laboraotry Press, Cold Spring Harbor, N.Y.
3. **al-Khodairy, F., E. Fotou, K. S. Sheldrick, D. J. Griffiths, A. R. Lehmann, and A. M. Carr.** 1994. Identification and characterization of new elements involved in checkpoint and feedback controls in fission yeast. Mol. Biol. Cell **5:**147–160.
4. **Bähler, J., J. Q. Wu, M. S. Longtine, N. G. Shah, A. McKenzie III, A. B. Steever, A. Wach, P. Philippsen, and J. R. Pringle.** 1998. Heterologous modules for efficient and versatile PCR-based gene targeting in *Schizosaccharomyces pombe*. Yeast **14:**943–951.
5. **Barnes, J. W., S. A. Tischkau, J. A. Barnes, J. W. Mitchell, P. W. Burgoon, J. R. Hickok, and M. U. Gillette.** 2003. Requirement of mammalian Timeless for circadian rhythmicity. Science **302:**439–442.
6. **Benard, M., C. Maric, and G. Pierron.** 2001. DNA replication-dependent formation of joint DNA molecules in Physarum polycephalum. Mol. Cell **7:**971–980.
7. **Boddy, M. N., B. Furnari, O. Mondesert, and P. Russell.** 1998. Replication checkpoint enforced by kinases Cds1 and Chk1. Science **280:**909–912.
8. **Boddy, M. N., P. H. Gaillard, W. H. McDonald, P. Shanahan, J. R. Yates III, and P. Russell.** 2001. Mus81-Eme1 are essential components of a Holliday junction resolvase. Cell **107:**537–548.
9. **Boddy, M. N., A. Lopez-Girona, P. Shanahan, H. Interthal, W. D. Heyer, and P. Russell.** 2000. Damage tolerance protein Mus81 associates with the FHA1 domain of checkpoint kinase Cds1. Mol. Cell. Biol. **20:**8758–8766.
10. **Boddy, M. N., and P. Russell.** 2001. DNA replication checkpoint. Curr. Biol. **11:**R953–R956.
11. **Brewer, B. J., and W. L. Fangman.** 1987. The localization of replication origins on ARS plasmids in *S. cerevisiae*. Cell **51:**463–471.
12. **Chan, R. C., A. Chan, M. Jeon, T. F. Wu, D. Pasqualone, A. E. Rougvie, and B. J. Meyer.** 2003. Chromosome cohesion is regulated by a clock gene paralogue TIM-1. Nature **424:**1002–1009.
13. **Dalgaard, J. Z., and A. J. Klar.** 2000. *swi1* and *swi3* perform imprinting, pausing, and termination of DNA replication in *S. pombe*. Cell **102:**745–751.
14. **Doe, C. L., J. S. Ahn, J. Dixon, and M. C. Whitby.** 2002. Mus81-Eme1 and Rqh1 involvement in processing stalled and collapsed replication forks. J. Biol. Chem. **277:**32753–32759.
15. **Du, L.-L., T. Nakamura, B. A. Moser, and P. Russell.** 2003. Retention but not recruitment of Crb2 at double-strand breaks requires Rad1 and Rad3 complexes. Mol. Cell. Biol. **23:**6150–6158.
16. **Fantes, P.** 1979. Epistatic gene interactions in the control of division in fission yeast. Nature **279:**428–430.
17. **Foss, E. J.** 2001. Tof1p regulates DNA damage responses during S phase in *Saccharomyces cerevisiae*. Genetics **157:**567–577.
18. **Friedberg, E. C., G. C. Walker, and W. Siede.** 1995. DNA repair and mutagenesis. ASM Press, Washington, D.C.
19. **Gaillard, P. H., E. Noguchi, P. Shanahan, and P. Russell.** 2003. The endogenous Mus81-Eme1 complex resolves Holliday junctions by a nick and counternick mechanism. Mol. Cell **12:**747–759.
20. **Gotter, A. L.** 2003. Tipin, a novel timeless-interacting protein, is developmentally co-expressed with timeless and disrupts its self-association. J. Mol. Biol. **331:**167–176.
21. **Grewal, S. I., and A. J. Klar.** 1997. A recombinationally repressed region between *mat2* and *mat3* loci shares homology to centromeric repeats and regulates directionality of mating-type switching in fission yeast. Genetics **146:**1221–1238.
22. **Gutz, H., and H. Schmidt.** 1985. Switching genes in *Schizosaccharomyces pombe*. Curr. Genet. **9:**325–331.
23. **Iino, Y., and M. Yamamoto.** 1997. The *Schizosaccharomyces pombe cdc6* gene encodes the catalytic subunit of DNA polymerase delta. Mol. Gen. Genet. **254:**93–97.
24. **Karthikeyan, R., E. J. Vonarx, A. F. Straffon, M. Simon, G. Faye, and B. A. Kunz.** 2000. Evidence from mutational specificity studies that yeast DNA polymerases delta and epsilon replicate different DNA strands at an intracellular replication fork. J. Mol. Biol. **299:**405–419.
25. **Katou, Y., Y. Kanoh, M. Bando, H. Noguchi, H. Tanaka, T. Ashikari, K. Sugimoto, and K. Shirahige.** 2003. S-phase checkpoint proteins Tof1 and Mrc1 form a stable replication-pausing complex. Nature **424:**1078–1083.
26. **Kaykov, A., A. M. Holmes, and B. Arcangioli.** 2004. Formation, maintenance and consequences of the imprint at the mating-type locus in fission yeast. EMBO J. **23:**930–938.
27. **Kearsey, S. E., S. Montgomery, K. Labib, and K. Lindner.** 2000. Chromatin binding of the fission yeast replication factor mcm4 occurs during anaphase and requires ORC and cdc18. EMBO J. **19:**1681–1690.
28. **Kim, S. M., and J. A. Huberman.** 2001. Regulation of replication timing in fission yeast. EMBO J. **20:**6115–6126.
29. **Kolodner, R. D., C. D. Putnam, and K. Myung.** 2002. Maintenance of genome stability in *Saccharomyces cerevisiae*. Science **297:**552–557.
30. **Krawchuk, M. D., and W. P. Wahls.** 1999. High-efficiency gene targeting in *Schizosaccharomyces pombe* using a modular, PCR-based approach with long tracts of flanking homology. Yeast **15:**1419–1427.
31. **Lindsay, H. D., D. J. Griffiths, R. J. Edwards, P. U. Christensen, J. M. Murray, F. Osman, N. Walworth, and A. M. Carr.** 1998. S-phase-specific activation of Cds1 kinase defines a subpathway of the checkpoint response in *Schizosaccharomyces pombe*. Genes Dev. **12:**382–395.
32. **Lopes, M., C. Cotta-Ramusino, G. Liberi, and M. Foiani.** 2003. Branch migrating sister chromatid junctions form at replication origins through Rad51/Rad52-independent mechanisms. Mol. Cell **12:**1499–1510.
33. **Lopes, M., C. Cotta-Ramusino, A. Pellicioli, G. Liberi, P. Plevani, M. Muzi-Falconi, C. S. Newlon, and M. Foiani.** 2001. The DNA replication checkpoint response stabilizes stalled replication forks. Nature **412:**557–561.
34. **MacQueen, A. J., and A. M. Villeneuve.** 2001. Nuclear reorganization and homologous chromosome pairing during meiotic prophase require *C. elegans* chk-2. Genes Dev. **15:**1674–1687.
35. **Mayer, M. L., I. Pot, M. Chang, H. Xu, V. Aneliunas, T. Kwok, R. Newitt, R. Aebersold, C. Boone, G. W. Brown, and P. Hieter.** 2004. Identification of protein complexes required for efficient sister chromatid cohesion. Mol. Biol. Cell **15:**1736–1745.
36. **McGlynn, P., and R. G. Lloyd.** 2002. Recombinational repair and restart of damaged replication forks. Nat. Rev. Mol. Cell Biol. **3:**859–870.
37. **Moreno, S., A. Klar, and P. Nurse.** 1991. Molecular genetic analysis of fission yeast *Schizosaccharomyces pombe*. Methods Enzymol. **194:**795–823.
38. **Muris, D. F., K. Vreeken, A. M. Carr, B. C. Broughton, A. R. Lehmann, P. H. Lohman, and A. Pastink.** 1993. Cloning the RAD51 homologue of *Schizosaccharomyces pombe*. Nucleic Acids Res. **21:**4586–4591.
39. **Muris, D. F., K. Vreeken, A. M. Carr, J. M. Murray, C. Smit, P. H. Lohman, and A. Pastink.** 1996. Isolation of the *Schizosaccharomyces pombe* RAD54 homologue, rhp54$^+$, a gene involved in the repair of radiation damage and replication fidelity. J. Cell Sci. **109:**73–81.
40. **Nasmyth, K., and P. Nurse.** 1981. Cell division cycle mutants altered in DNA replication and mitosis in the fission yeast *Schizosaccharomyces pombe*. Mol. Gen. Genet. **182:**119–124.
41. **Noguchi, E., C. Noguchi, L. L. Du, and P. Russell.** 2003. Swi1 prevents replication fork collapse and controls checkpoint kinase Cds1. Mol. Cell. Biol. **23:**7861–7874.
42. **Ogawa, Y., T. Takahashi, and H. Masukata.** 1999. Association of fission yeast Orp1 and Mcm6 proteins with chromosomal replication origins. Mol. Cell. Biol. **19:**7228–7236.
43. **Osborn, A. J., and S. J. Elledge.** 2003. Mrc1 is a replication fork component whose phosphorylation in response to DNA replication stress activates Rad53. Genes Dev. **17:**1755–1767.
44. **Osborn, A. J., S. J. Elledge, and L. Zou.** 2002. Checking on the fork: the DNA-replication stress-response pathway. Trends Cell Biol. **12:**509–516.
45. **Osman, F., J. Dixon, C. L. Doe, and M. C. Whitby.** 2003. Generating crossovers by resolution of nicked Holliday junctions: a role for Mus81-Eme1 in meiosis. Mol. Cell **12:**761–774.
46. **Ostermann, K., A. Lorentz, and H. Schmidt.** 1993. The fission yeast *rad22* gene, having a function in mating-type switching and repair of DNA damages, encodes a protein homolog to Rad52 of *Saccharomyces cerevisiae*. Nucleic Acids Res. **21:**5940–5944.
47. **Paques, F., and J. Haber.** 1999. Multiple pathways of recombination induced by double-strand breaks in *Saccharomyces cerevisiae*. Microbiol. Mol. Biol. Rev. **63:**349–404.

48. **Pavlov, Y. I., C. S. Newlon, and T. A. Kunkel.** 2002. Yeast origins establish a strand bias for replicational mutagenesis. Mol. Cell **10:**207–213.
49. **Rabitsch, K. P., A. Toth, M. Galova, A. Schleiffer, G. Schaffner, E. Aigner, C. Rupp, A. M. Penkner, A. C. Moreno-Borchart, M. Primig, R. E. Esposito, F. Klein, M. Knop, and K. Nasmyth.** 2001. A screen for genes required for meiosis and spore formation based on whole-genome expression. Curr. Biol. **11:**1001–1009.
50. **Rigaut, G., A. Shevchenko, B. Rutz, M. Wilm, M. Mann, and B. Seraphin.** 1999. A generic protein purification method for protein complex characterization and proteome exploration. Nat. Biotechnol. **17:**1030–1032.
51. **Sanchez, J. A., S. M. Kim, and J. A. Huberman.** 1998. Ribosomal DNA replication in the fission yeast, *Schizosaccharomyces pombe*. Exp. Cell Res. **238:**220–230.
52. **Schmidt, H., P. Kapitza, and H. Gutz.** 1987. Switching genes in *Schizosaccharomyces pombe*: their influence on cell viability and recombination. Curr. Genet. **11:**303–308.
53. **Segurado, M., M. Gomez, and F. Antequera.** 2002. Increased recombination intermediates and homologous integration hot spots at DNA replication origins. Mol. Cell **10:**907–916.
54. **Shcherbakova, P. V., and Y. I. Pavlov.** 1996. 3′→5′ exonucleases of DNA polymerases epsilon and delta correct base analog induced DNA replication errors on opposite DNA strands in *Saccharomyces cerevisiae*. Genetics **142:** 717–726.
55. **Sogo, J. M., M. Lopes, and M. Foiani.** 2002. Fork reversal and ssDNA accumulation at stalled replication forks owing to checkpoint defects. Science **297:**599–602.
56. **Stewart, E., C. R. Chapman, F. Al-Khodairy, A. M. Carr, and T. Enoch.** 1997. *rqh1*$^+$, a fission yeast gene related to the Bloom's and Werner's syndrome genes, is required for reversible S phase arrest. EMBO J. **16:**2682–2692.
57. **Tanaka, K., and P. Russell.** 2001. Mrc1 channels the DNA replication arrest signal to checkpoint kinase Cds1. Nat. Cell Biol. **3:**966–972.
58. **Tercero, J. A., and J. F. Diffley.** 2001. Regulation of DNA replication fork progression through damaged DNA by the Mec1/Rad53 checkpoint. Nature **412:**553–557.
59. **Uetz, P., L. Giot, G. Cagney, T. A. Mansfield, R. S. Judson, J. R. Knight, D. Lockshon, V. Narayan, M. Srinivasan, P. Pochart, A. Qureshi-Emili, Y. Li, B. Godwin, D. Conover, T. Kalbfleisch, G. Vijayadamodar, M. Yang, M. Johnston, S. Fields, and J. M. Rothberg.** 2000. A comprehensive analysis of protein-protein interactions in *Saccharomyces cerevisiae*. Nature **403:**623–627.
60. **Vengrova, S., S. Codlin, and J. Z. Dalgaard.** 2002. RTS1—an eukaryotic terminator of replication. Int. J. Biochem. Cell Biol. **34:**1031–1034.
61. **Vengrova, S., and J. Z. Dalgaard.** 2004. RNase-sensitive DNA modification(s) initiates *S. pombe* mating-type switching. Genes Dev. **18:**794–804.
62. **Virgin, J. B., J. P. Bailey, F. Hasteh, J. Neville, A. Cole, and G. Tromp.** 2001. Crossing over is rarely associated with mitotic intragenic recombination in *Schizosaccharomyces pombe*. Genetics **157:**63–77.
63. **Waga, S., and B. Stillman.** 1998. The DNA replication fork in eukaryotic cells. Annu. Rev. Biochem. **67:**721–751.
64. **Warren, C. D., D. M. Eckley, M. S. Lee, J. S. Hanna, A. Hughes, B. Peyser, C. Jie, R. Irizarry, and F. A. Spencer.** 2004. S-phase checkpoint genes safeguard high-fidelity sister chromatid cohesion. Mol. Biol. Cell **15:**1724–1735.
65. **Washburn, M. P., D. Wolters, and J. R. Yates III.** 2001. Large-scale analysis of the yeast proteome by multidimensional protein identification technology. Nat. Biotechnol. **19:**242–247.
66. **Wellinger, R. E., P. Schar, and J. M. Sogo.** 2003. Rad52-independent accumulation of joint circular minichromosomes during S phase in *Saccharomyces cerevisiae*. Mol. Cell. Biol. **23:**6363–6372.
67. **Woodgate, R.** 1999. A plethora of lesion-replicating DNA polymerases. Genes Dev. **13:**2191–2195.
68. **Yanow, S. K., Z. Lygerou, and P. Nurse.** 2001. Expression of Cdc18/Cdc6 and Cdt1 during G_2 phase induces initiation of DNA replication. EMBO J. **20:**4648–4656.
69. **Yonemasu, R., S. J. McCready, J. M. Murray, F. Osman, M. Takao, K. Yamamoto, A. R. Lehmann, and A. Yasui.** 1997. Characterization of the alternative excision repair pathway of UV-damaged DNA in *Schizosaccharomyces pombe*. Nucleic Acids Res. **25:**1553–1558.
70. **Zou, H., and R. Rothstein.** 1997. Holliday junctions accumulate in replication mutants via a RecA homolog-independent mechanism. Cell **90:**87–96.